Vibrational and Pure Nuclear Quadrupole Resonance Spectra of Hexahalometalates[1]

Theodore L. Brown, W. Gordon McDugle, Jr.,[2a] and L. Gregory Kent[2b]

Contribution from the Materials Research Laboratory and Noyes Chemical Laboratory, University of Illinois, Urbana, Illinois 61801. Received October 22, 1969

Abstract: The ^{35}Cl and ^{81}Br nuclear quadrupole resonance frequencies are reported for a large number of hexahalometal systems. Resonances at 27° reported for the first time (in MHz) are: CsNbCl$_6$ (8.59, 8.25), CsTaCl$_6$ (9.12, 8.80), KWCl$_6$ (11.46, 11.34), RbWCl$_6$ (11.56, 11.32), CsWCl$_6$ (11.75, 11.60, 11.28), Rb$_2$WCl$_6$ (10.58), Cs$_2$WCl$_6$ (10.91), MoCl$_5$ (14.08), Cs$_2$MoCl$_6$ (10.74), K$_3$MoCl$_6$ (9.83, 9.54), Cs$_2$SnCl$_6$ (16.06), Cs$_2$TeCl$_6$ (15.67), WBr$_6$ (72.12), Cs$_2$WBr$_6$ (75.29), K$_2$OsBr$_6$ (111.78), (NH$_4$)$_2$OsBr$_6$ (112.78), Cs$_2$OsBr$_6$ (116.84), Cs$_2$SnBr$_6$ (110.00). Infrared and Raman spectra are reported for a number of chlorides of W(IV), W(V), Ta(V), and Nb(V). Metal–halogen bonding is discussed in terms of σ and π contributions to covalency. Quantities derived from various spectroscopic data, particularly vibrational and nqr, are consistent with the model proposed. This model differs from earlier descriptions of third-row metal–halogen bonds in that account is taken of variation in effective electronegativity of the metal.

Numerous infrared and Raman vibrational spectra, and halogen pure nuclear quadrupole resonance spectra, have accumulated for hexahalo compounds of the heavy transition elements in varying oxidation states. Although certain trends are evident in the results from each technique, the effects of changes in metal oxidation states, as opposed to changes in 5d orbital occupancies in a given oxidation state, have not been clearly elucidated. The purpose of this contribution is to present new vibrational and nuclear quadrupole resonance data, to derive a self-consistent set of force constants from all available vibrational data, and to relate force constant variations to the halogen quadrupole coupling constants in terms of a suitable model for metal–halogen bonding.

Theoretical Considerations

The quadrupole coupling constant, eQq, for quadrupolar nuclei is determined by the expectation value for the one-electron operator, q. This consists of a nuclear part, computed classically, and an electronic part, q_e, at nucleus k.

$$q_e^k = \left\langle \Psi^* \left| \sum_\sigma \frac{3\cos^2\theta_{\sigma k} - 1}{r_{\sigma k}^3} \right| \Psi \right\rangle \quad (1)$$

From this fact, it follows that eQq is determinable from a knowledge of the geometry and ground-state wave function for the system containing the nucleus of interest. In general, because there are problems in evaluating the details of effects arising from core electrons, it is common to relate the values of eQq for halogens to those characteristic of the free halogen atom.[3-5]

$$|eQq|_{mol} = U_p|eQq|_{atom} \quad (2)$$

The factor U_p is, for chlorine at least, determined predominantly by populations in the 3p orbitals

$$U_p = \frac{1}{2}(N_{p_x} + N_{p_y}) - N_{p_z} \quad (3)$$

where the N's refer to electron populations in the chlorine 3p orbitals. The p_z orbital is directed along the bond axis; p_x and p_y are normal to it. In the absence of π bonding from chlorine to a bonded atom capable of π-acceptor action, N_{p_x} and N_{p_y} should each be very nearly 2. Thus, U_p is a measure of a *difference* in p-orbital occupancies. As the difference decreases, either because of increasing M–X bond polarity, or because of π bonding from X to M, the observed quadrupole resonance frequency decreases. Various models, but most particularly that due to Townes and Dailey,[3] have been employed in attempts to relate the one observable, eQq_{mol}, to bond parameters such as ionic character, π bonding, and hybridization. In the MCl$_6{}^{2-}$ series, Kubo, Nakamura, and coworkers have measured a number of resonances[6] and have related variations in eQq mainly to variation in π bonding from $3p_\pi$ orbitals of chlorine to the metal $5d_\pi$ orbitals. The extent of π bonding has been assumed to be proportional to the number of holes in the t_{2g} set of metal 5d orbitals. The availability of procedures for generating molecular orbital wave functions for such systems provides a route for computing q_{zz} directly, after suitable simplifications to eq 1. Thus, Cotton and Harris[7] have been able to obtain charge distributions in ReCl$_6{}^{2-}$, OsCl$_6{}^{2-}$, IrCl$_6{}^{2-}$, and PtCl$_6{}^{2-}$ which lead to reasonably good agreement between calculated and observed eQq. The agreement with Kubo and Nakamura's conclusions with respect to variation in metal charge and variation in extent of chlorine–metal π bonding is, however, not particularly good, as discussed below.

(3) C. H. Townes and B. P. Dailey, *J. Chem. Phys.*, 17, 782 (1949).
(4) C. T. O'Konski, "Physical Methods in Determination of Organic Structures," Vol. II, F. C. Nachod and W. D. Phillips, Ed., Academic Press, New York, N. Y., 1962, Chapter 11.
(5) E. A. C. Lucken, "Nuclear Quadrupole Coupling Constants," Academic Press, London, 1969.

(6) M. Kubo and D. Nakamura, *Advan. Inorg. Chem. Radiochem.*, 8, 257 (1966).
(7) F. A. Cotton and C. B. Harris, *Inorg. Chem.*, 6, 376 (1967).

The quadratic bond stretching force constant, F, is not directly relatable to the expectation value for a one-electron operator. The relationship between F and q involves terms which require knowledge of how the molecular charge distribution varies as a function of the motions of the nuclei. For example, Salem[8] has obtained an expression for the stretching of the bond in an A–B diatomic molecule (with B at the center of the coordinate system).

$$F = Z_A \left[q_{zz}(A) + \frac{4}{3} \pi \rho(A) - \int \frac{\partial \rho}{\partial X_A} \frac{\cos \theta_A}{r_A{}^2} d\tau \right] \quad (4)$$

The first term in this expression is the field gradient at nucleus A due to all charges external to it. In the second term $\rho(A)$ is the one-electron charge distribution at nucleus A. The third term relates to the readjustment of charge density due to movement of nucleus A. Development of expressions such as this for use in molecules of interest, other than MH bonds, is extremely difficult. Some form of variational and/or perturbational approach is required to deal with the third term. Depending on the form of the approximate wave functions used in evaluation, various nonequivalent equations can be obtained by holding different sets of electronic coordinates constant during differentiation.[9] For the present, therefore, it would appear that the direct computation of stretching force constants by solving the Roothaan SCF molecular eigenvalue problem for a number of points on the nuclear coordinate surface provides the best means of approaching a rigorous calculation of stretching force constants. Because such a calculation is prohibitively costly for any but the simplest molecules, there is strong interest in a more empirical approach which might relate the bond stretching force constants to properties of the ground-state molecule. A model recently developed by Borkman and Parr is of particular interest in this regard.[10,11]

The quadratic force constant, F, for a stretching of the diatomic A–B bond is given by

$$F = \frac{2D_e + 2T^\infty{}_{val}}{R_e{}^2} \quad (5)$$

where D_e is the dissociation energy for A–B, and $T^\infty{}_{val}$ is the kinetic energy of the "valence" electrons at $R = \infty$. This latter quantity can be related to the bond valence electrons by suitable partitioning of the electrons between the two atoms, and the valence orbitals involved on each. Borkman and Parr show that eq 5 can be taken as a relationship between F and the number of valence electrons in the bond region. There is in principle nothing to preclude application to an individual bond in a polyatomic molecule. Further, the details of the model are not very sensitive to variations in bond polarity. This model provides a basis for predicting variations in M–X stretching force constants in $MX_6{}^n$ systems.

In $MX_6{}^n$ species at the same value of n, the effective M–X bond order and M–X distance should be essentially constant for a series of closely related M. In the series $n = -2$, the M–Cl distances in compounds

crystallizing in the K_2PtCl_6 arrangement vary in the heavy metal series from 2.37 Å for K_2ReCl_6 to 2.50 Å for Cs_2PbCl_6.[12] M–Cl distances within this range are found for the Zr, Ti, Mo, Se, and Te compounds also. It seems clear, therefore, that bond length variations are not responsible for large variations in MCl stretching force constant. Furthermore, one expects that the overall charge on the metal will not vary greatly in the heavy metal series from $WCl_6{}^{2-}$ to $PtCl_6{}^{2-}$. Variation in metal 5d orbital occupancies in this series, which should lead to variation in chlorine-metal π bonding, should therefore be compensated to considerable degree by an oppositely directed variation in polarity of the σ bond. In this sense the π bonding between chlorine and metal is "sacrificial," in that covalency which arises through π bonding is, to a large degree, probably compensated for by increased polarity in the σ bond. If we assume as an approximation that overlap in the π orbitals makes the same contribution to bonding as the σ overlap, we conclude that the metal–halogen stretching force constants should be a measure of the overall bonding charge density in the M–Cl bond in the series. The quadrupole coupling constant at chlorine, however, changes greatly in the same series, because of changes in the *relative* values of N_{p_z} and N_{p_x}, N_{p_y}.

The series involving the same metal or closely related metals in different oxidation states requires different considerations. It is intuitively obvious that in the series WCl_6, $WCl_6{}^-$, $WCl_6{}^{2-}$, for example, the binding of chlorine to metal should decrease in the order listed, and the M–Cl bond distance should exhibit a concomitant increase. On the basis of the considerations involved in eq 5, the M–Cl stretching force constant should decrease with decreasing formal oxidation state of the metal.

It is not so clear just how the quadrupole coupling constant at chlorine should vary, since the observable relates primarily to a *difference* in σ- and π-orbital populations. In the series WCl_6, $WCl_6{}^-$, and $WCl_6{}^{2-}$, the d-orbital configurations are d^0, d^1, and d^2, respectively. Presumably, chlorine-to-metal π bonding decreases with increasing 5d orbital occupancy. On the other hand, there should also be some increase in σ-bond polarity, *i.e.*, decrease in σ-bond order, because of the decrease in formal metal charge. There does not appear to be an *a priori* way to quantitatively assess the change in bonding in cases such as these, but a careful examination of stretching force constant and halogen quadrupole coupling constant variations should provide an informative picture.

Results

Vibrational Spectra. The infrared and Raman spectra of $MX_6{}^n$ systems (X = Cl, Br) have been extensively reported upon.[13-15] The Raman spectra have been of particular interest since the advent of laser sources. For an MX_6 species of O_h symmetry six distinct frequencies are expected. Typical normal coordinates are depicted in a number of places.[16,17] Only the two T_{1u}

(8) L. Salem, *J. Chem. Phys.*, **38**, 1227 (1963).
(9) M. L. Benston and B. Kirtman, *ibid.*, **44**, 119 (1966).
(10) R. F. Borkman and R. G. Parr, *ibid.*, **48**, 1116 (1968).
(11) R. F. Borkman, G. Simons, and R. G. Parr, *ibid.*, **50**, 58 (1969).

(12) R. W. G. Wyckoff, "Crystal Structures," Vol. 3, 2nd ed, Interscience Publishers, New York, N. Y., 1965.
(13) R. J. H. Clark, "Halogen Chemistry," Vol. 3, Academic Press, New York, N. Y., 1967, pp 85–121.
(14) D. W. James and M. J. Nolan, *Progr. Inorg. Chem.*, **9**, 195 (1968).
(15) R. E. Hester, *Coord. Chem. Rev.*, **2**, 319 (1967).

modes are infrared active. The T_{2u} mode is neither infrared nor Raman active. The remaining three modes are Raman active.

The second and third transition row metal (IV) hexachlorides most frequently crystallize in the K_2PtCl_6 cubic structure, thus preserving the MX_6^{2-} ion symmetry. There might in principle be a dynamic, or even a static, Jahn–Teller distortion in certain of these systems,[18] but no evidence for such distortion has been adduced from vibrational data on chloro systems. Electronic degeneracy occurring in the T_{2g} d-orbital levels is not expected to lead to a large effect, so that a static distortion would not be expected in any case.

The corresponding metal(V) compounds do not generally adopt a cubic structure. $CsNbCl_6$,[19] $CsTaCl_6$,[19] and $CsWCl_6$[20] are isostructural and of low symmetry. In both WCl_6^- and $MoCl_6^-$, manifestations of distortion in the solid substances[21] may arise primarily through lattice effects.[22]

Solid WCl_6 is observed in rhombohedral solid modification, involving only slightly distorted WCl_6 octahedra.[23] The W–Cl bond distance is 2.24 Å in the solid, 2.26 Å in the gas phase.

For lack of suitable solvents it has often been necessary to employ Raman and infrared data for the solid compounds in normal coordinate analyses of MX_6^n systems. Where the site symmetry is lower than O_h it might be expected that splittings in certain bands will occur, but these are generally not large and an average value for the frequency should be adequate in a force field analysis. More seriously, the effect of cation size, and the relationship of the solid-state frequencies to solution data, need to be considered. In general, variations in the frequency of a particular mode are not large. A systematic decrease in M–Cl stretching force constant with cation size has been noted for $PtCl_6^{2-}$ salts.[24] For K^+, Rb^+, Cs^+, and $(C_2H_5)_4N^+$, F calculated for a modified Urey–Bradley force field varies monotonically from 1.83 to 1.73 mdyn/Å. This may be regarded as typical behavior.

We have attempted to assemble a set of vibrational data for various MCl_6^n systems which in our view represent the most self-consistent set, in terms of minimizing divergences due to lattice effects, cation size, solvent effect, etc. These are collected in Table I.[25–35]

(16) K. Nakamoto, "Infrared Spectra of Inorganic and Coordination Compounds," John Wiley & Sons, Inc., New York, N. Y., 1963, p 118.
(17) G. Herzberg, "Infrared and Raman Spectra," D. Van Nostrand Co., Inc., New York, N. Y., 1945, p 122.
(18) B. Weinstock and G. L. Goodman, *Advan. Chem. Phys.*, 11, 169 (1965).
(19) K. W. Bagnall and D. Brown, *J. Chem. Soc.*, 3021 (1964).
(20) K. W. Bagnall, D. Brown, and J. G. H. DuPreez, *ibid.*, 2603 (1964).
(21) R. A. Walton, P. C. Crouch, and B. J. Brisdon, *Spectrochim. Acta*, 24A, 601 (1968).
(22) R. D. Dowsing and J. F. Gibson, *J. Chem. Soc.*, A, 655 (1967).
(23) J. A. A. Ketelaar and G. W. Van Oosterhout, *Rec. Trav. Chim. Pays-Bas*, 62, 197 (1943).
(24) D. M. Adams and D. M. Morris, *J. Chem. Soc.*, A, 1666 (1967).
(25) W. Van Bronswyk, R. J. H. Clark, and L. Maresca, *Inorg. Chem.*, 8, 1395 (1969).
(26) S. M. Horner, R. J. H. Clark, B. Crociani, D. B. Copley, W. W. Horner, F. N. Collier, and S. Y. Tyree, *ibid.*, 7, 1859 (1968).
(27) L. A. Woodward and M. J. Ware, *Spectrochim. Acta*, 20, 711 (1964).
(28) P. J. Hendra and P. J. D. Park, *ibid.*, 23A, 1635 (1967).
(29) D. M. Adams and H. A. Gebbie, *ibid.*, 19, 925 (1963).
(30) L. A. Woodward and J. A. Creighton, *ibid.*, 17, 594 (1967).
(31) J. A. Creighton and L. A. Woodward, *Trans. Faraday Soc.*, 58, 1077 (1962).
(32) D. M. Adams and D. M. Morris, *J. Chem. Soc.*, A, 1669 (1967).

Table I. Compilation of Characteristic Vibrational Frequencies of ML_6^n Species[a] (cm⁻¹)

Ion	ν_1	ν_2	ν_3	ν_4	ν_5
$HfCl_6^{2-}$ [b]	326	257	275	145	156
$TaCl_6^{2-}$ [c]			297	160	
WCl_6^{2-} [d]			303	167	
$ReCl_6^{2-}$	346[e]	(275)[f]	313[g]	172[g]	159[e]
$OsCl_6^{2-}$	346[e]	(274)[f]	314[g]	177[g]	165[e]
$IrCl_6^{2-}$ [h]	352	(225)	333[i]	184[i,j]	190
$PtCl_6^{2-}$ [k]	344	320			162
$PtCl_6^{2-}$ [l]	340	135	325	181	160
$PbCl_6^{2-}$ [m]	285	212			137
$PbCl_6^{2-}$ [n]	281	209	262	142	139
$SnCl_6^{2-}$ [o]	311	229	303	166	158
WCl_6^- [d]	378	318	330	158	
$TaCl_6^-$ [p]	378	298	330	158	180
$NbCl_6^-$ [q]	368	288	333	162	183
WCl_6 [r]	437	331	373	160	182
WCl_6 [s]	409	317			209

[a] Frequencies determined by observation of combination bands are given in parentheses. [b] Spectra of solid $[(C_2H_5)_4N]_2HfCl_6$.[25] [c] Solid Cs_2TaCl_6.[26] [d] Present work; see Table II. [e] Aqueous solution.[27] [f] Calculated from $\nu_2 + \nu_3$, observed for solid Cs_2MCl_6.[27] [g] Infrared spectrum of solid cesium salt.[27] [h] Raman spectrum of solid K_2IrCl_6.[28] [i] Solid K_2IrCl_6.[29] [j] We have remeasured the lower frequency infrared absorption and found it to be at 180 cm⁻¹, essentially in agreement with Adams and Gebbie.[29] [k] Aqueous solution.[30] [l] Solid $[(C_2H_5)_4N]_2PtCl_6$.[24] [m] Aqueous solution.[31] [n] Solid $[(C_2H_5)_4N]_2PbCl_6$.[32] [o] Raman spectrum of aqueous solution;[33a] infrared spectrum of solid $[(CH_3)_4N]_2SnCl_6$.[33b] [p] Raman spectrum of CH_3NO_2 solution of $(CH_3)_4NTaCl_6$ and solid $(C_2H_5)_4NTaCl_6$ (footnote d) agree well with the results of Clark, et al.,[25] except for ν_2, which they report at 298 cm⁻¹; their value seems the more reliable. [q] Table II and ref 25 and 26. [r] Table II. The Raman results for WCl_6 in CH_3NO_2 solution are in reasonable agreement with the solid-state results, and the infrared results, for CCl_4 solution, are in close agreement with the solid[25] and solution[34,35] results. [s] WCl_6 in liquid Cl_2 solution.[35]

The criteria followed have been: (a) whenever available, solution data are employed; (b) where solid-state data must be employed, those pertaining to the largest cation are preferable. We have made both Raman and infrared measurements on a number of systems; the results are summarized in Table II, and some of the data as applicable are incorporated in Table I.

Because the observables relating to the vibrational potential are limited, the force fields employed in a normal coordinate analysis must be limited also in terms of the number of variables. Modified valence and modified Urey–Bradley force fields, MVFF and MUBFF, respectively, have been employed in this work. The program due to Schachtschneider and Snyder[36] was employed in carrying out the calculations to provide a least-squares fit between observed and calculated frequencies. The MVFF force field is of the form

$$V = \frac{1}{2}\left[F_r \sum_i^6 r_i^2 + r_0^2 F_\alpha \sum \alpha_{ij} + 2F_t \sum_{i \neq k} r_i r_k + F_c \sum_{i \neq j} r_i r_j + r_0 F_{r\alpha} \sum r_i \alpha_{ij} \right] \quad (6)$$

where F_r refers to the M–Cl bond stretching, F_α to Cl–M–Cl angle bending, F_t to the interaction of *trans* M–Cl stretchings, F_c to the interaction of *cis* M–Cl

(33) (a) L. A. Woodward and L. E. Anderson, *ibid.*, 1284 (1957); (b) I. Wharf and D. F. Shriver, *Inorg. Chem.*, 8, 914 (1969).
(34) J. C. Evans and G. Y. S. Lo, *J. Mol. Spectrosc.*, 23, 147 (1968).
(35) J. A. Creighton, *Chem. Commun.*, 163 (1969).
(36) J. H. Schachtschneider and R. G. Snyder, *Spectrochim. Acta*, 19, 85, 117 (1963).

Table II. Infrared (ν_3, ν_4, ν(lattice)) and Raman (ν_1, ν_2, ν_5) Spectra of $MCl_n{}^n$ Species[a]

Compound	ν_1	ν_2	ν_3	ν_4	ν_5	ν(lattice)
$WCl_6{}^b$	437	331 (vw)	373^c / 368^d	158^c / 167^d	182	
$CsWCl_6{}^{e,f}$			327 (s)	167 (m)		57 (w)
$(CH_3)_4NWCl_6{}^{b,e}$	378	318	330 (s)	158 (m)		75 (vw)
$(C_2H_5)_4NWCl_6{}^{b,e}$	378	318	319 (s) / 330 (w)	159 (m)		63 (vw)
$K_2WCl_6{}^e$			324 (s)	165 (m)		77 (w)
$Rb_2WCl_6{}^e$			311 (s)	165 (m)		70 (w)
$Cs_2WCl_6{}^e$			303 (s)	167 (m)		67 (w)
$(CH_3)_4NTaCl_6{}^{b,e,g}$	378		303 (s)	160 (m)	180	
$(C_2H_5)_4NTaCl_6{}^h$	378 (s)	326 (vw)			180 (w)	
$CsTaCl_6{}^e$			317 (s)	156 (m)		
$(CH_3)_4NNbCl_6{}^{e,i}$			337 (s)	164 (m)		
$CsNbCl_6{}^{b,e,i}$	370		340 (s)	168 (m)	183 (vw)	
$(C_2H_5)_4NNbCl_6{}^h$	367					

[a] The symbols s, m, w, and vw in parentheses following the listed frequencies refer to observations of relative intensities as strong, medium, weak, or very weak, respectively. [b] Raman spectrum in nitromethane solution. [c] CCl_4 and CH_2Cl_2 solutions. [d] Cyclohexane solution. [e] Infrared spectrum as Nujol mull. [f] At 77°K, on a polyethylene support, ν_4 is split: 153, 169 cm^{-1}. [g] At 77°K, a weak shoulder at 300 cm^{-1} and a weak absorption at 386 cm^{-1} are seen in the infrared spectrum. [h] Raman spectrum of a single crystal. [i] A weak shoulder is seen at 369 cm^{-1} in the infrared spectrum of $(CH_3)_4NNbCl_6$ and at 365 cm^{-1} for $CsNbCl_6$.

stretchings, and $F_{r\alpha}$ to the interaction between an M–Cl_i stretching and the bending of an angle of which M–Cl_i forms one side. Several bend–bend and bend–stretch interaction constants have been set equal to zero. In the decision to neglect bend–bend interactions, we differ from Van Bronswyk, Clark, and Maresca, who include certain terms of this kind.[25] The matter of principal interest for our purposes is the metal–halogen stretching force constant. Whatever the merits of including additional interaction force constants, with consequent necessary constraints on the relative values of some of the force constants employed, such variations do not significantly affect the relative M–Cl stretching force constants in a series of related species.[37]

The MUBFF employed is similar to that described by Hiraishi, Nakagawa, and Shimanouchi;[38] the bend–bend interaction constant is assumed to be zero, and separate cis and trans stretch–stretch interaction constants, k_c and k_t, respectively, are included. Following the usual practice, F' is taken as $-0.1F$. The symmetry force constants based on the two modified force fields are given in Table III.[39]

Table III. Symmetry Force Constants

Modified valence force field	Modified Urey–Bradley force field[39]
A$_{1g}$	
$F_{11} = F_r + 4F_c + F_t$	$F_{11} = K + 4F + k_t + 4k_c$
$F_{22} = F_r - 2F_c + F_t$	$F_{22} = K + F + 3F' + 2k_t - 2k_c$
T$_{1u}$	
$\begin{vmatrix} (F_r - F_t) & (-2F_{r\alpha}) \\ (-2F_{r\alpha}) & (F_\alpha) \end{vmatrix}$	$\begin{vmatrix} (K + 2F + 2F' - k_t) & (F + F') \\ (F + F') & (H + F/2 - 3F'/2) \end{vmatrix}$
T$_{2g}$	
$F_{55} = F_\alpha$	$F_{55} = H + F/2 - F'/2$
T$_{2u}$	
$F_{66} = F_\alpha$	$F_{66} = H + F/2 - F'/2$

The results of application of the two force fields to the vibrational data of Table I are shown in Tables IV

(37) J. N. Murrell, *J. Chem. Soc., A*, 297 (1969).
(38) J. Hiraishi, I. Nakagawa, and T. Shimanouchi, *Spectrochim. Acta*, **20**, 819 (1964).
(39) H. Kim, P. A. Souder, and H. H. Claassen, *J. Mol. Spectrosc.*, **26**, 46 (1968).

Table IV. Modified Valence Force Field Constants

Species	F_r	F_c	F_t	F_α	$F_{r\alpha}$	ν_6 (calcd), cm^{-1}
$HfCl_6{}^{2-}$	1.45	0.14	0.23	0.13	0.047	113
$ReCl_6{}^{2-}$	1.71	0.15	0.18	0.15	0.042	122
$OsCl_6{}^{2-}$	1.72	0.14	0.16	0.19	0.05	
$IrCl_6{}^{2-}$ ^{a}	1.66	0.26	−0.094	0.20	0.060	140
$IrCl_6{}^{2-}$ ^{b}	1.78	0.20	0.02	0.20	0.06	140
$PtCl_6{}^{2-}$	1.91	0.06	0.26	0.16	0.042	124
$NbCl_6{}^-$	1.79	0.18	0.31	0.16	0.073	125
$TaCl_6{}^-$	1.93	0.19	0.30	0.17	0.022	122
$WCl_6{}^-$ ^{c}	2.05	0.14	0.28	0.17	0.05	127
$WCl_6{}^0$ ^{d}	2.44	0.28	0.41	0.18	−0.01	130
$WCl_6{}^0$ ^{e}	2.14	0.23	0.42	0.23	−0.08	147
$SnCl_6{}^{2-}$	1.53	0.15	0.05	0.18	0.10	119
$PbCl_6{}^{2-}$	1.13	0.12	0.024	0.11	0.03	105

[a] Assuming $\nu_2 = 225$ cm^{-1}. [b] Assuming $\nu_2 = 260$ cm^{-1}. [c] Based on "best choice of F_α and $F_{r\alpha}$; see text. [d] CH_3NO_2 solution Raman data (see Table I). [e] Cl_2 solution Raman data (see Table I).

Table V. Modified Urey–Bradley Force Constants for $MCl_6{}^n$ Species Based on the Frequencies of Table I

Ion	K	F	H	k_t	k_c	ν_6 (calcd)
$HfCl_6{}^{2-}$	1.25	0.045	0.11	0.33	0.11	112
$ReCl_6{}^{2-}$	1.45	0.16	0.06	0.15	0.06	114
$OsCl_6{}^{2-}$	1.46	0.15	0.08	0.14	0.07	119
$IrCl_6{}^{2-}$ ^{a}	1.52	0.057	0.17	−0.057	0.22	139
$IrCl_6{}^{2-}$ ^{b}	1.61	0.08	0.16	0.047	0.15	137
$PtCl_6{}^{2-}$	1.59	0.22	0.039	0.21	−0.062	114
$PbCl_6{}^{2-}$	0.91	0.13	0.037	0.003	0.048	97
$SnCl_6{}^{2-}$	0.99	0.26	0.03	−0.05	0.05	106
$WCl_6{}^-$ ^{c}	1.86	0.10	0.10	0.36	0.10	119
$TaCl_6{}^-$	1.55	0.13	0.10	0.44	0.11	125
$NbCl_6{}^-$	1.45	0.18	0.048	0.31	0.080	
$WCl_6{}^d$	2.15	0.22	0.045	0.30	0.16	117
$WCl_6{}^e$	2.04	0.19	0.082	0.17	0.13	127

[a] Assuming $\nu_2 = 225$ cm^{-1}. [b] Assuming $\nu_2 = 260$ cm^{-1}. [c] Assuming $H = 0.10$. [d] Based on CH_3NO_2 solution Raman data (Table I). [e] Based on Cl_2 solution Raman data (Table I).

and V. For $WCl_6{}^-$, only four frequencies are observed. It was therefore necessary to make some further assumptions about the force field to complete the calculation. Fortunately, the missing frequency is related to the bending motions. In view of the uniformity

observed in $F_{r\alpha}$ and F_α in the MVFF results, it seems reasonable to assume a value for either F_α or $F_{r\alpha}$, and examine the resulting effect on the remaining force constants. The effect proved to be very slight; 2.05, 0.28, and 0.14 were chosen as the most reasonable values for F, F_t, and F_c, respectively. These were obtained for $F_\alpha = 0.17$, $F_{r\alpha} = 0.05$.

The data for $WCl_6{}^{2-}$ and $TaCl_6{}^{2-}$ are too incomplete to permit more than an indirect comparison with the results for the other $MCl_6{}^{2-}$ species. It is unfortunate that ν_2 has not been observed for $ReCl_6{}^{2-}$, $OsCl_6{}^{2-}$, and $IrCl_6{}^{2-}$. The value assigned[28] for ν_2 of $IrCl_6{}^{2-}$ seems incorrect; if ν_2 is omitted from the MVFF calculation and F_α or $F_{r\alpha}$ fixed at a value in the range observed for all other $MCl_6{}^{2-}$ species, it is possible to calculate force constants; these, of course, are very much in line with the values calculated for $ReCl_6{}^{2-}$ and $OsCl_6{}^{2-}$. A value of 260 cm^{-1} is predicted for ν_2 from these results. Although it is obviously a questionable point at present, our view is that 260 cm^{-1} is a more reasonable expectation than the 225-cm^{-1} value assigned from the presumed combination band. We therefore show MVFF and MUBFF results for $IrCl_6{}^{2-}$ assuming both 225 and 260 cm^{-1} for ν_2.

Nuclear Quadrupole Resonance Spectra. A number of new halogen quadrupole resonances are reported here for the first time. In addition, careful frequency measurements at a number of temperatures have been made on a wide range of chloride and bromide compounds. These measurements are to be discussed in another publication. Table VI lists those results which

Table VI. [35]Cl and Br Nuclear Quadrupole Resonances at 300°K (MHz)

NbCl₅	13.06	*MoCl₅*	*14.08*
CsNbCl₆	*8.59,*	*Cs₂MoCl₆*	*10.74*
	8.25	*K₃MoCl₆*	*9.83,*
			9.54
TaCl₅	13.39		
CsTaCl₆	*9.12,*		
	8.80	K₂OsCl₆	16.82
		K₂IrCl₆	20.73
WCl₆	10.54	K₂PtCl₆	25.77
KWCl₆	*11.46,*	Cs₂PtCl₆	26.55
	11.34		
RbWCl₆	*11.56,*		
	11.32		
CsWCl₆	*11.75,*		
	11.60,		
	11.28		
K₂WCl₆	10.19	K₂SnCl₆	15.06
Rb₂WCl₆	*10.58*	Rb₂SnCl₆	15.60
Cs₂WCl₆	*10.91*	(NH₄)₂SnCl₆	15.48
K₂ReCl₆	13.88	*Cs₂SnCl₆*	*16.06*
Cs₂ReCl₆	14.59	(NH₄)₂PbCl₆	17.06
		(NH₄)₂TeCl₆	14.99
		Cs₂TeCl₆	*15.67*
WBr₆	*72.12*	*K₂OsBr₆*	*111.78*
Cs₂WBr₆	*75.29*	*(NH₄)₂OsBr₆*	*112.78*
K₂ReBr₆	94.13	*Cs₂OsBr₆*	*116.83*
		K₂PtBr₆	167.25
		Cs₂PtBr₆	173.18
		(NH₄)₂PtBr₆	169.1
		Cs₂SnBr₆	*110.00*

are of immediate use in the present work. The values have all been obtained in our laboratories, but only those in italics are the first values reported for the compound. The reader is referred to recent reviews[5,6]
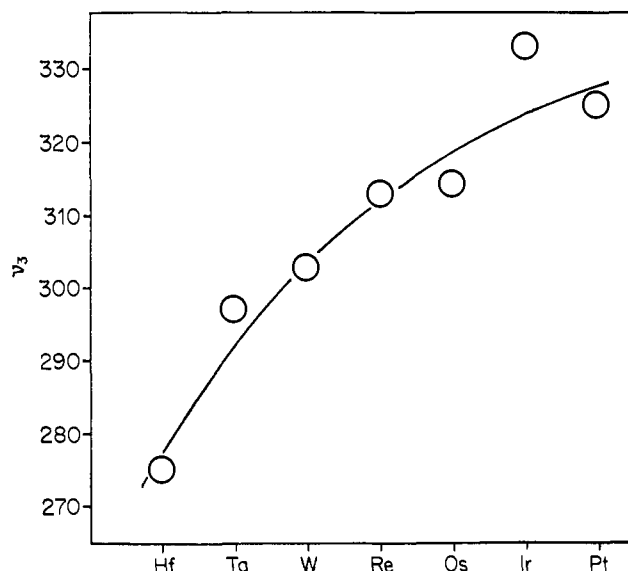

Figure 1. Variation in ν_3 as a function of atomic number for $MCl_6{}^{2-}$ species.

for references to earlier work on systems previously reported by others.

Although variation in cation does occasion some variation in resonance frequency for a given anion, the variations are usually small in relation to the differences between two anions of the same charge and cation, but differing in d-orbital populations. It would be preferable to employ data for a lower temperature, but there are severe difficulties in obtaining low-temperature spectra for many of the compounds. Accordingly, the room-temperature values seem the best choice.

Discussion

Empirical Force Constant Relationships. It is evident from the results displayed in Tables IV and V that the same general trends in force constant results are observed using either the MVFF or MUBFF force fields. We will, therefore, restrict our discussion to the results displayed in Table IV. On the basis of the frequency variations noted for certain of the normal modes, as well as on the basis of the force field results, the M–Cl stretching force constant increases monotonically in the series extending from $HfCl_6{}^{2-}$ to $PtCl_6{}^{2-}$. This is particularly evident in the variations in ν_3 and ν_4 for which the data are most extensive, and possibly most reliable. Figure 1 displays the variation in ν_3 for $MCl_6{}^{2-}$ ions as a function of atomic number. Figure 2 displays F as a function of the number of 5d electrons in the same series, and for the hexachlorotungstates. We conclude that there is a definite, though not large, increase in metal–chlorine stretching force constant with increasing atomic number in the $MCl_6{}^{2-}$ series. Although there are insufficient data to determine the stretching force constant for $WCl_6{}^{2-}$, it seems reasonable, on the basis of Figures 1 and 2, to assume a value of 1.6 mdyn/Å for this quantity.

While the increase in force constant with the increasing atomic number in the metal(IV) series is not very large, a much more noticeable effect is seen with an increase in oxidation state in the $WCl_6{}^{2-}$, $WCl_6{}^-$, WCl_6 series. The sharp increase in stretching force constant with increasing oxidation state of the central metal can be interpreted in terms of increased bonding inter-
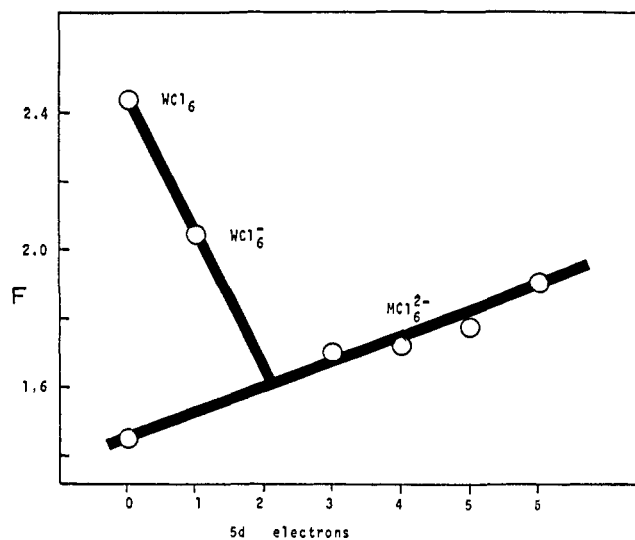
Figure 2. Variation in M–Cl stretching force constant, F, from modified valence force field, as a function of 5d-orbital occupancy for $MCl_6{}^n$ systems.

action between the halogen and metal and is the expected result in terms of the considerations involved in eq 5. The increased force constant is presumably the result of both increased electron density in the bonding region and decreased metal–halogen bond distance.

The origin of increasing F with increasing atomic number in the metal(IV) series can be interpreted in terms of an increase in total charge in the bonding region. Presumably the increased electron density in the bonding region is the result of an increase in effective metal nuclear charge, as seen by the halogen, with increasing atomic number. In this connection, it is of interest that the present results are in accord with Jørgensen's ideas[40] regarding increase in "optical" electronegativity with increasing atomic number in this series. Jørgensen's values are derived from consideration of the energies of the charge-transfer electronic transitions, in which an electron is transferred from the π orbital largely localized on the halogens to an orbital which is largely metal d_π in character. These optical electronegativities actually reflect the variation in energy of the d_π atomic orbitals on the metal in the series. These energies, in turn, reflect the changing effective nuclear charge at the metal.

Analysis of Nqr Data. As mentioned in the introductory section the electric field gradient, q, can be determined from a knowledge of the ground-state charge distribution and of the equilibrium nuclear configuration. Thus, if one begins with, let us say, an approximate molecular orbital description for an $MX_6{}^n$ species, one can, using eq 1, determine the electronic contribution to the electric field gradient. In practice, a number of approximations are made.[41,42] The core electrons are assumed merely to cancel a certain number of nuclear charges. Advantage is taken of the $1/r^3$ dependence of the operator to discard terms which involve distances greater than one bond distance. After approximating a number of the remaining

(40) (a) C. K. Jørgensen, *Advan. Chem. Phys.*, **5**, 33 (1963); (b) "Orbitals in Atoms and Molecules," Academic Press, New York, N. Y., 1962, Chapter 7.
(41) E. Scrocco, *Advan. Chem. Phys.*, **5**, 319 (1963).
(42) F. A. Cotton and C. B. Harris, *Proc. Nat. Acad. Sci. U. S.*, **56**, 12 (1966).

integrals, one is generally left with an expression involving orbital populations on the atom in question, and overlap populations in the immediate vicinity. Thus, an approximate molecular orbital approach generally reduces to the Townes and Dailey approach, with the difference that empirically determined parameters such as ionicity, π bonding, and covalency are now implicit in the coefficients of the orbitals employed as basis set, in the occupied molecular orbitals.

The Townes and Dailey approach is not basically different from this so-called molecular orbital approach. In the latter case, one begins with an approximate description of the electron distribution based on a prior calculation. In the Townes and Dailey approach, one sets up the formalism for expressing eQq in terms of whatever description of the local charge distribution (*i.e.*, estimates of 3p orbital occupancies in the case of chlorine) one has available. It is of interest, therefore, to continue attempts to estimate the populations of the chlorine 3p orbitals on the basis of various spectroscopic results. In the present case, we can attempt to reconcile data or quantities from three spectroscopic methods. The experimental values for eQq provide a direct measure of the difference in the p_z and p_x, p_y orbital occupancies. The stretching force constant, F, on the other hand, provides a measure of the total bonding electronic charge in the M–Cl bond. Thirdly, the "optical electronegativities" of Jørgensen relate to the effective energy of the d_π orbital on the metal atom.

If we now assume a hybridization factor for the halogen in these compounds, we can proceed with an analysis similar to that employed previously. The convention of assuming 15% s character in the chlorine–metal σ bond appears reasonable in terms of the orbital populations obtained by Cotton and Harris[7] for a series of heavy metal(IV) hexachlorides. Assuming this quantity for all of the compounds studied here, the orbital populations are expressed as

$$N_{p_x} = 2 - \pi/2 \tag{7}$$

$$N_{p_y} = 2 - \pi/2 \tag{8}$$

$$N_{p_z} = 2 - (1 - S)\sigma = 2 - 0.85\sigma \tag{9}$$

These equations coupled with eq 2 and 3 yield the following

$$= \frac{|eQq|_{mol}}{|eQq|_{atom}} = -\pi/2 + 0.85\sigma \tag{10}$$

If we assume that $\sigma + \pi$ represents the covalency in the M–Cl bond, the charge p on the metal is given by the formal charge, j, less the sum of the covalencies: $p = j - 6(\sigma + \pi)$.

In their analysis of the halogen quadrupole coupling constant results for heavy metal halides, Kubo and Nakamura[6] assume that the extent of π bonding between halogen and the metal is directly related to the number of holes or vacancies in the d_π metal orbitals. Thus, assuming that there is a 0.054 π-bond character in the Ir–Cl bond, on the basis of the esr results,[43] the extent of π bonding is taken to be a simple multiple of this for the elements to the left of iridium, depending upon the number of d_π orbital holes. Jørgensen's con-

(43) (a) J. H. E. Griffiths and J. Owen, *Proc. Roy. Soc.*, A226, 96 (1954); (b) J. H. E. Griffiths, J. Owen, and I. M. Ward, *ibid.*, A219, 526 (1953).

Table VII. Bonding Parameters in MCl_6^n Systems from Nuclear Quadrupole Resonance Data

	Pt(IV)	Ir(IV)	Os(IV)	Re(IV)	W(IV)	W(V)	W(VI)
d_π holes	0	1	2	3	4	5	6
χ_{opt}	2.7	2.4	2.2	2.0	1.7	2.0	2.1
f	0.47	0.379	0.308	0.253	0.186	0.208	0.193
π	0	0.054	0.081	0.097	0.100	0.16	0.21
σ	0.55	0.48	0.41	0.35	0.28	0.34	0.35
Metal charge, p	0.70	0.80	1.06	1.34	1.72	2.0	2.6

siderations would suggest, however, that this simple assumption is not warranted. Rather, since the optical electronegativity of the metal decreases relative to halogen as one proceeds to the left of platinum, the number of π electrons transferred per d_π orbital hole should in fact decrease. If one were to assume that the number of electrons transferred per d_π orbital hole were inversely proportional to the difference in optical electronegativities, and assuming that the value for $IrCl_6{}^{2-}$ is correctly assessed to be 0.054 electron per halogen, the values for π charge transferred to the metal per halogen are as follows.

$$\pi_M = 0.054n(\Delta\chi_{Ir}/\Delta\chi_M) \qquad (11)$$

$$\Delta\chi_M = \chi^M{}_{opt} - \chi^{Cl} \qquad (12)$$

Although the assumption that π-electron transfer from halogen to metal is conditioned by the difference in optical electronegativities is empirical, it is more reasonable than to assume that there is no variation in this quantity with change in metal.

In Table VII are listed the values of χ_{opt}, as given by Jørgensen for the (IV) oxidation states, and by Walton, Crouch, and Brisdon for tungsten in various oxidation states.[44] The values of f are based on the nqr data for the K^+ salts (Table VI), and the π values are computed from eq 11 and 12, using $\chi_{Cl} = 3.0$. The σ values are then obtained using eq 10. The net charge on the metal calculated in this manner agrees almost perfectly with the molecular orbital calculations of Cotton and Harris,[7] although the variation in σ and π contributions obtained in the MO work is much smaller than indicated in Table VII. The metal charge does not remain essentially constant throughout the series, as in the results obtained by Kubo and Nakamura, but, rather, the lighter metals possess a significantly larger net positive charge.

The analysis shows the expected marked increase in the extent of π bonding with increasing metal charge in the $WCl_6{}^n$ series. The remarkably small variation in eQq for chlorine in the three tungsten halides is ascribable to more or less parallel increases in the extent of both σ and π bonding with increasing metal charge. The net charge on the metal, of course, also increases, but at a rate considerably less than the increase in formal charge.

A relationship between Jørgensen's optical electronegativities and ^{35}Cl nqr frequencies in the metal(IV) hexachlorides has been discussed recently by Machmer.[45] His treatment is, however, quite unlike ours in that he notes only a gross correlation between χ_{opt} and nqr frequencies and makes no attempt to distinguish π-bonding from σ-bonding effects. His correlation

completely breaks down for changes in metal oxidation state involving the same coordination number, as in the W(VI), W(V), W(IV) series.

It is not obvious, a priori, that the variation in M–Cl stretching force constant in the metal(IV) series can be associated entirely with variation in covalency, since highly polar bonds also possess substantial force constants as the result of the electrostatic interactions between the charged atoms. Nevertheless, the present analysis of the nqr results for the metal(IV) series supports our interpretation of the force constant results; the gradually increasing M–Cl stretching force constant can be associated with an increased covalency in the metal-chlorine bond. In this connection the present results are in agreement with the trend observed by Fenske and Radtke,[46] relating an increased total metal–chlorine overlap population in $MCl_4{}^n$ species to increase in frequency of the T_2 M–Cl stretching mode. It is not so obvious in the W(IV)–W(V)–W(VI) series that the increase in W–Cl stretching force constant is relatable only to covalency, since the formal charge on the metal is also increasing. Furthermore, it may be doubted whether the present use of optical electronegativities may be pushed so far as to make possible a comparison of W(VI) with, for example, Pt(IV). On the basis of the results presented here, one would need to conclude that total covalency, as represented by the sum of $\sigma + \pi$, is about the same for WCl_6 as for $PtCl_6{}^{2-}$. It seems safe at least to conclude that, within a series of related species such as the (IV) metals, or in the tungsten series with varying oxidation states, such comparisons as outlined above are valid.

The constancy in chlorine quadrupole coupling constant with change of metal oxidation state noted above for the tungsten compounds is seen also in the results for molybdenum(IV) and -(III). It is interesting to note also that the second transition row compounds compare very closely in value of chlorine quadrupole coupling constant with the analogous third-row compounds, e.g., $NbCl_5$–$TaCl_5$ and Cs_2MoCl_6–Cs_2WCl_6.

The analogous bromide complexes of the third-row transition elements behave very similarly to the chloride complexes with respect to all of the relationships outlined above (Table VI). It is particularly interesting that the relative constancy of halogen quadrupole coupling constant with varying oxidation state of tungsten is seen also in the bromide series: $WBr_6 = 72.19$ MHz, $Cs_2WBr_6 = 75.29$ MHz.

The d^{10} metal(IV) chloro complexes exhibit halogen quadrupole coupling constants comparable to those for the transition series, but the metal-chlorine stretching force constants are significantly lower. There is, of course, no significant degree of π bonding between halogen and metal in these compounds. eQq is thus

(44) R. A. Walton, P. C. Crouch, and B. J. Brisdon, Spectrochim. Acta, 24A, 601 (1968).

(45) P. Machmer, Z. Naturforsch., 24b, 193 (1969).

(46) R. F. Fenske and D. D. Radtke, Inorg. Chem., 7, 479 (1968).

mainly a measure of σ covalency. The lower force constant observed can be traced, via eq 5, to an increased metal–chlorine bond distance but, more importantly, to a smaller net covalency in the M–Cl bond.

To summarize, the present analysis of halogen quadrupole coupling constant and metal–chlorine stretching force constant data suggests that in the series of metal(IV) hexachloro complexes extending from $HfCl_6{}^{2-}$ to $PtCl_6{}^{2-}$ the metal charge decreases substantially, as a result of increased covalency in the metal–halogen bond. The analysis suggests that the degree of π bonding per metal d_π orbital vacancy increases in this series, and that σ covalency also increases. The increase in total covalent bonding is responsible for a gradual increase in metal–chlorine stretching force constant. In the series $WCl_6{}^n$ ($n = -2, -1, 0$) an increase in formal charge on the central metal is accompanied by an essentially constant quadrupole coupling constant at the halogen, as a result of concomitant increases in covalency in both σ and π orbitals. The net total increase in covalency, coupled with increased formal metal charge, is responsible for a substantial increase in metal–chlorine stretching force constant in this series.

Experimental Section

A. Preparation of Materials. Cs_2HfCl_6. Swirl 4.5 g of $HfCl_4$ into about 30 ml of concentrated HCl, avoiding much increase in temperature. Vigorous liberation of gas is normal. Pour the acid mixture into a solution of 4.5 g of CsCl in 30 ml of concentrated HCl, with stirring. Filter. Wash twice with 10 ml of HCl, five times with acetone, and three times with ether. Vacuum dry at 80° for 15 min. *Anal.* Calcd: Hf, 27.17. Found: Hf, 27.20.

Cs_2MoCl_6. Under dry nitrogen atmosphere grind 2.75 g of Mo_2Cl_{10} (sublimed) with 3.35 g of CsCl. Add a fivefold volume of ICl, refluxing at about 120° in a 100-ml round-bottom flask for 24 hr. Stir at least twice during that time. Evacuate at 150° for 4 days. Wash five times with carbon tetrachloride which has been stored over molecular sieves, then five times with methylene chloride, stored similarly. Dry by passing nitrogen through the fritted glass filter for 5 min while stirring the powder. *Anal.* Calcd: Cl, 37.05. Found: Cl, 36.56.

WBr_6. Load 5 g of $W(CO)_6$, crushed, into the top half of a Schlenk apparatus. Flush with nitrogen. Place 10 g of bromine into the bottom half, also flushing with nitrogen. Evacuate partially, opening the top half of the apparatus to a nitrogen-flushed oil bubbler. As the evolution of CO slows, gradually warm the bromine, maintaining it at about 70° for 3 days. Evacuate the Schlenk apparatus, freeing it of bromine, and transfer to a dry nitrogen atmosphere. Place the WBr_6 into a heat-sealable vial. *Anal.* Calcd: W, 27.0; Br, 73.0. Found: W, 28.70; Br, 71.56.

(K, Rb, Cs)WCl_6. The method used is essentially that of Dickinson and coworkers,[47] replacing their sealed tube with a 50-ml round-bottom flask open to about 1 atm of nitrogen. Periodic regrinding with an additional gram of WCl_6 is necessary. The Soxhlet extractor, flushed with nitrogen, is operated until the carbon tetrachloride efflux is colorless. The sample is evacuated and sealed at 80°. *Anal.* Calcd for $RbWCl_6$: Cl, 44.20. Found: Cl, 43.95.

(K, Rb, Cs)$_2WCl_6$. The method used is essentially that of Kennedy and Peacock.[48] The reactions were carried out in a nitrogen atmosphere. The cesium salt, instead of undergoing long evacuation at 290°, is removed from the nitrogen atmosphere after 1 hr of high-temperature evacuation and is washed with chloroform, water, acetone, and ether, each three times. The sample is air-dried. *Anal.* Calcd for K_2WCl_6: Cl, 44.80. Found: Cl, 44.65. Calcd for Cs_2WCl_6: Cl, 32.10. Found: Cl, 30.52.

Cs_2WBr_6. Under dry nitrogen, grind together 9 g of WBr_6 and 5.4 g of CsI. Heat at 100° in a 50-ml round-bottom flask for 3 days. Then evacuate for 2 days at 290°. Remove the system

from the dry nitrogen atmosphere. Wash and dry as for Cs_2WCl_6. *Anal.* Calcd: W, 19.80; Br, 51.60. Found: W, 19.70; Br, 49.73.

R_4NWCl_6. WCl_6, purified by repeated sublimation, is added to $SOCl_2$, followed by addition of a twofold molar excess of R_4NCl. The R_4NWCl_6 salts are crystallized from the solution. *Anal.* Calcd for $(CH_3)_4NWCl_6$: C, 10.21; H, 2.55; Cl, 45.19. Found: C, 10.32; H, 2.87; Cl, 44.86. Calcd for $(C_2H_5)_4NWCl_6$: C, 18.24; H, 3.80; Cl, 40.39; W, 34.91. Found: C, 18.67; H, 3.82; Cl, 40.18; W, 35.57. Both tetraalkylammonium salts exhibit a high solubility in $SOCl_2$. Fairly large crystals of $(C_2H_5)_4NWCl_6$ can be grown by slow evaporation of the solvent.

$TaCl_6{}^-$ and $NbCl_6{}^-$ Compounds. These were prepared as described by Bagnall and Brown.[49] *Anal.* Calcd for $CsTaCl_6$: Cl, 40.48. Found: Cl, 40.68. Calcd for $(CH_3)_4NTaCl_6$: C, 10.27; H, 2.59; Cl, 45.47. Found: C, 10.57; H, 2.64; Cl, 45.42. Calcd for $(C_2H_5)_4NTaCl_6$: C, 18.34; H, 3.82; Cl, 40.62. Found: C, 18.95; H, 4.07; Cl, 40.86. Calcd for $CsNbCl_6$: Cl, 48.51. Found: Cl, 48.19.

Cs_2SnCl_6. Swirl a solution of 0.015 mol of $SnCl_4 \cdot 5H_2O$ in a minimum of HCl into a solution of 0.04 mol of CsCl in a minimum of HCl; filter; wash five times with acetone and five times with ether. *Anal.* Calcd: Cl, 35.66. Found: Cl, 36.08.

Cs_2SnBr_6. Boil 4.4 g of $SnBr_4$ in 50 ml of HBr for 1 hr. Cool. Swirl this mixture into a solution of 6 g of CsBr in 20 ml of HBr. Filter. Wash three times with HBr, ten times with absolute ethanol, and five times with ether. *Anal.* Calcd: Br, 55.50. Found: Br, 55.20.

Cs_2PbCl_6. Dissolve $Pb(OAc)_4$ in concentrated HCl at about 30°. Chlorine evolution and precipitate formation occur. Swirl the filtrate into excess CsCl dissolved in HCl. Filter; wash five times with acetone and three times with ether. Vacuum dry at 70°.

(K, Cs)$_2ReCl_6$. Boil 5 g of $KReO_4$ and 15 ml of H_3PO_2 for 2 hr in 250 ml of HCl. The original yellow color turns to green, then fades to light green. Evacuate the hot system to one-half volume. Add a solution of 0.04 mol of metal chloride (3.0 g of KCl or 6.0 g of CsCl) dissolved in a minimum of HCl. Cool to produce copious precipitation; filter; wash five times each with acetone and ether. *Anal.* Calcd for K_2ReCl_6: Cl, 44.65. Found: Cl, 43.06. Calcd for Cs_2ReCl_6: Cl, 32.0. Found: Cl, 32.55.

K_2ReBr_6. Boil 2.5 g of $KReO_4$ and 7 ml of H_3PO_2 for 16 hr in 125 ml of HBr; then add, hot, to a solution of 2.4 g of KBr in 100 ml of HBr. Cool to 0°, filter, then wash five times with absolute ethanol and five times with ether. Color changes during the initial boiling parallel those for $ReCl_6{}^{2-}$, going from yellow to red, fading to pink. *Anal.* Calcd: Br, 64.50. Found: Br, 63.46.

Cs_2ReBr_6. Prepare as above, but use 4.0 g of CsBr. The cooling step is not essential. *Anal.* Calcd: Br, 51.50. Found: Br, 51.42.

H_2OsCl_6. Break a 1.0-g vial (0.00394 mol) of OsO_4 (caution: volatile, toxic) into a 500-ml round-bottom flask (RBF) containing 300 ml of HCl; boil for 16 hr with the Glas-col heater set at 50 V; decant the solution from the pieces of broken glass. Allow the 150-ml volume of liquid to cool. Volume reduction may be accomplished with the aid of reduced pressure after at least 5 hr of boiling at 1 atm.

K_2OsCl_6. To the above H_2OsCl_6 solution add 1.0 g of powdered KCl; boil, reducing the volume, until the first crystals appear. The house vacuum may be used after all KCl is in solution. Cool slowly to 0°. Wash five times with acetone and three times with ether. Caution: avoid local heating at any step. Osmium reduction occurs, evidenced by particles of the metal (black) throughout the solution. *Anal.* Calcd: Cl, 44.30. Found: Cl, 44.14.

Cs_2OsCl_6. Prepare as above, but add the metal chloride predissolved (1.7 g of CsCl in a minimum of HCl). Prefiltration cooling is unnecessary. *Anal.* Calcd: Cl, 31.83. Found: Cl, 31.30.

H_2OsBr_6. Break a 1.0-g vial of OsO_4 (see above) into 50 ml of concentrated HBr; boil for 2 hr; decant from broken glass, rinsing with another 50 ml of HBr. Boil to 50 ml, avoiding local heating. Allow the solution to cool.

K_2OsBr_6. Boil the above solution with 1.7 g of powdered KBr; after the KBr is in solution, reduce the volume to about 30 ml using vacuum. Avoid hotspot reduction of osmium. Cool to $-40°$, filter, wash five times each in absolute ethanol and ether. Avoid

(47) R. N. Dickinson, S. E. Feil, E. N. Collier, W. W. Horner, S. M. Horner, and S. Y. Tyree, *Inorg. Chem.*, 3, 1600 (1964).
(48) C. D. Kennedy and R. D. Peacock, *J. Chem. Soc.*, 3392 (1963).

(49) K. W. Bagnall and D. Brown, *ibid.*, 3021 (1964).

acetone. Dry. Winnow away any light chaff. *Anal.* Calcd: Br, 64.15. Found: Br, 64.20.

Cs₂OsBr₆. To the hexabromoosmate ion solution above, add a solution of 2.0 g of CsBr in a minimum of HBr. Filter. Wash five times each in absolute ethanol and ether. *Anal.* Calcd: Br, 51.30. Found: Br, 51.50.

K₂PtCl₆. Dissolve 8 g of H₂PtCl₆·6H₂O (0.015 mol) in a minimum quantity of warm HCl. Swirl it into a solution of 3 g of KCl in a minimum of HCl. Cool slowly to just below room temperature; filter; wash crystals, while crushing, six times in acetone and four times in ether. *Anal.* Calcd: Cl, 43.78. Found: Cl, 43.58.

Cs₂PtCl₆. Into acidic hexachloroplatinate, as above, stir a solution of 5.0 g of CsCl in 30 ml of HCl. Filter the product. Boil it in 10 volumes of water; filter again; wash five times with acetone and three times with ether. *Anal.* Calcd: Cl, 31.60. Found: Cl, 31.68.

K₂PtBr₆. Boil 5 g of H₂PtCl₆·6H₂O for several hours in 250 ml of HBr, reducing the system, at 1 atm, to one-half volume, lowering pressure toward the end to avoid "hotspot" reduction of Pt(IV). Pour this into a solution of 2.5 g of KBr dissolved in a minimum quantity of hot KBr. Cool to 25°; filter; wash five times with acetone and three times with ether. *Anal.* Calcd: Br, 63.65. Found: Br, 63.69.

Cs₂PtBr₆. Into acidic hexabromoplatinate, as above, pour a solution of 4.8 g of CsBr in 25 ml of HBr; filter. Boil the solid in 10 volumes of water; wash, with crushing, in acetone five times and then three times in ether. *Anal.* Calcd: Br, 51.00. Found: Br, 50.60.

A number of samples for which results are reported in Table VII were received from commercial sources, and were purified, where volatile, by repeated sublimations. K₃MoCl₆ was used as received from Climax Molybdenum Co.

B. Nuclear Quadrupole Resonance Apparatus. A self-quenched superregenerative oscillator is operated with feedback provided by connection of the cathode of a triode 6C4 to a center tap on the radiofrequency tank coil. This arrangement affords maximum frequency range for any continuous scan. The coherence level of the oscillator is maintained within the range necessary for maximum signal-to-noise output by comparing the random (incoherence) noise issuing from the oscillator in a narrow band about 500 Hz with a preset norm, and using the deviation from that norm to control a servo-driven potentiometer, which, in turn, provides a variable current to the oscillator's grid. Signal output from the oscillator is obtained by application of a 100-Hz sinusoidal Zeeman magnetic field to the sample, normal to the radiofrequency magnetic field. Phase-sensitive detection is accomplished with a Princeton Applied Research Model HR-8, with integrator time constant operated at 10 sec, with a 12-db/octave rolloff.

Heating and cooling of samples is accomplished using single-pass nitrogen gas systems.

Frequency measurements are made with the use of a Drake Model 2-B communications receiver and crystal converters. During each scan, oscillator carrier and side bands can be monitored. An accuracy of 1 kHz is attainable in favorable cases, *i.e.*, when there are not closely spaced multiple resonances, but normally measurements are made to within ± 10 kHz.

C. Vibrational Spectra. Infrared measurements were made with a Beckman IR-11 spectrophotometer, frequency-calibrated using water vapor. The measurements were generally made on Nujol mulls prepared in either a glove bag or an inert atmosphere enclosure. Room-temperature spectra were recorded with the mulls mounted on high-pressure polyethylene sheet. A cryostat was employed to record spectra at liquid nitrogen temperature. High density polyethylene was employed as window material. The sample was mounted on a suitable support at the end of a copper block which was in contact with the liquid N₂ reservoir. CsI, silicon, and polyethylene were employed as low-temperature supports. (The polyethylene is not very useful as a support in low-temperature work because of its poor heat transfer characteristics.)

Raman spectra were recorded on a Perkin-Elmer LR-2 laser Raman spectrometer, fitted with a 4-MW He-Ne source. Standard solid sample mounting techniques were employed.

Electronic and Vibrational Spectroscopy in a Nematic Liquid Crystal Solvent. Band Polarizations for Binuclear Metal Carbonyls

Robert A. Levenson, Harry B. Gray, and Gerald P. Ceasar

Contribution No. 3957 from the Arthur Amos Noyes Laboratory of Chemical Physics, California Institute of Technology, Pasadena, California 91109. Received October 6, 1969

Abstract: A new technique for obtaining the polarizations of infrared and electronic absorption bands is discussed in detail and illustrated by application to certain binuclear metal carbonyls of the type M₂(CO)₁₀. In this method orientation is achieved by dissolving the molecule of interest in a nematic liquid crystal host which is subsequently aligned by a simple rubbing procedure. Infrared polarization data for the binuclear metal carbonyls in nematic solution rigorously establish the assignments of the C≡O stretching bands. The infrared results also determine that the sign of the ordering factor S_{zz}, which describes solute orientation, is positive, indicating parallel alignment of the M₂(CO)₁₀ molecules with the nematic host. The degree of orientation obtained by the simple rubbing procedure used in these experiments is comparable to that achieved in liquid crystal nmr experiments. The polarized electronic spectra of Mn₂(CO)₁₀ in nematic solution show that the first very intense band is polarized along the metal-metal bond. The band is assigned $d\sigma(M-M) \rightarrow d\sigma^*(M-M)$.

Knowledge of polarizations of absorption bands in the ultraviolet, visible, and infrared regions of the spectrum is an invaluable aid in the elucidation of transition assignments. Numerous methods exist to determine band polarizations; among them are single-crystal techniques (both absorption[1] and reflection[2]), photoselection,[3] stretched films,[4] and cholesteric-liquid-crys-

(1) D. S. McClure, *Solid State Phys.*, **8**, 1 (1959); **9**, 399 (1959); H. C. Wolf, *ibid.*, **9**, 1 (1959).
(2) B. G. Anex, *Mol. Cryst.*, **1**, 1 (1966).